Progress of Theoretical Physics, Vol. 94, No. 2, August 1995

A New Type of Irregular Motion in a Class of Game Dynamics Systems

Tsuyoshi CHAWANYA*

Yukawa Institute for Theoretical Physics, Kyoto University, Kyoto 606-01

(Received May 22, 1995)

The asymptotic behavior of the orbits in the vicinity of the networks of heteroclinic orbits is analyzed using an approximation. As a result of the analysis, the existence of a new type of asymptotic behavior in a game dynamics system is discovered. The feature of this asymptotic behavior is a combination of the chaotic motion and the attraction to a heteroclinic cycle; the trajectory visits several unstable stationary states repeatedly with an irregular order, and the typical length of stays near the steady states grows roughly exponentially with the number of visits. The dynamics underlying this irregular motion is related to the low-dimensional chaotic dynamics. The relation of this irregular motion with a peculiar type of instability of heteroclinic cycle attractors is also examined.

§ 1. Introduction

It is well known that heteroclinic cycles can generically exist in a certain class of model systems. For example, the structurally stable heteroclinic cycle is found in the Lotka-Volterra equation system,[1] and several model systems with symmetry.[2)~6)] The heteroclinic orbits can form more complicated structure than a simple cycle.[7),8)] Some interesting phenomena are reported concerning such networks,[9),8)] however, the property of the flow in the vicinity of the network is not fully understood yet.

In this paper, we will analyze the flow of the game dynamics systems by introducing a truncated equation of motion which is valid in the neighborhood of heteroclinic networks. The analysis shows that the motion in the vicinity of the network has no characteristic time scale, and that there exist a new type of asymptotic behavior. The feature of the behavior is a combination of the attraction to a heteroclinic cycle and a chaotic motion; the orbits visit some of the saddles with an irregular order with geometrically expanding length of the stays. The irregularity in the sequence of the visited saddles is related to a deterministic chaotic dynamics and not due to the randomness from noise. The behavior is robust against a small variation of the parameters.

§ 2. Model equation and the structure of the phase space

The game dynamics system we will study is a kind of population dynamics, and is represented with a set of equations,

$$\frac{d}{dt}x_i=(\sum_{j=1}^{n}g_{ij}x_j-\sum_{j=1}^{n}\sum_{k=1}^{n}g_{jk}x_jx_k)x_i \tag{1}$$

with constraints,

*) Present address: Research Institute of Electorical Communication, Tohoku University, Sendai 980-77, Japan.

$$\sum_{i=1}^{n} x_i=1 . \quad (0 \le x_i \le 1) \qquad (2)$$

x_i represents the renormalized population of species i. $\{g_{ij}\}$ defines the interaction between species, each g_{ij} representing the score of species i in its battle with j.

Such a model was proposed by Taylor and Jonker in the context of the evolution of strategy into ESS (evolutionary stable states);[10] it is also regarded as a simplified model equation for the molecular evolution,[11] and gives a minimal model for the system of interacting self replicators.[12] It is also related to the Lotka-Volterra equation through a transformation of variables.[12]

Several types of asymptotic behavior are known to exist for this system. The simplest one is the relaxation to a resting state. Chaotic oscillations as well as regular oscillations can be observed in some range of parameters when 4 or more components are involved.[13)~15)] Attractive heteroclinic cycles are observed generically for systems with 3 or more components.[1] In such cases, the orbit stays relatively long in the vicinity of the saddles and then move towards another saddle. An example of temporal evolution of x_i for this type of behavior is exhibited in Fig. 1. Our target phenomenon contains the attraction to a heteroclinic cycle attractor as the simplest case.

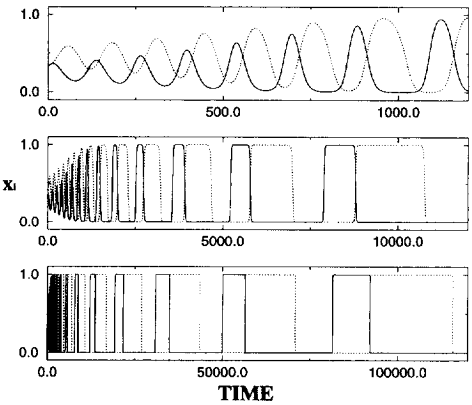

Fig. 1. An example of the orbit being attracted to a heteroclinic cycle. This figure exhibits the behavior of the orbit observed in a game dynamics system with 3 components. The parameters are set as

$$g_{ij}=\begin{pmatrix} 0.0 & -0.09 & 0.12 \\ 0.1 & 0.0 & -0.1 \\ -0.11 & 0.05 & 0.0 \end{pmatrix},$$

and the initial condition is set as $x_1=x_2=x_3=1/3$. The abscissa represents the time, and the ordinate represents the value of x_i. Two components are plotted with solid lines (x_1) and with dotted lines (x_2). All the three boxes are associated with the same orbit, but the scale of time is different. The length of the stays near the quasi stable states gets longer and longer, while the length of the transition does not change.

As is easily seen from the constraint (2), the phase space of the game dynamics system with n components is given by an $(n-1)$-dimensional simplex. The surface of the simplex consists of n hyper-planes represented by $x_i=0$ $(i=1, \cdots, n)$, each of which is an $(n-2)$-dimensional flow-invariant simplex, surrounded by $(n-1)$ of $(n-3)$-dimensional flow-invariant simplexes. The flow on such an invariant simplex can be described by a game dynamics equation of the original form but with a reduced number of components.

Although there can exist many fixed points in the phase space of this system, there exists at most only one fixed point in the interior of the phase space in generic cases. It is because the stationary condition $\sum_j g_{ij} x_j = C$ (C is an arbitrary constant which does not depend on i) together with the constraint $\sum x_i=1$ determines unique $\boldsymbol{x} \equiv (x_1, \cdots, x_n)$ and C, if $\{g_{ij}\}$ is not degenerated.

Consequently we can specify an arbitrary fixed point by specifying a set of components with non-zero value, because the fixed point should be in the interior of the phase space of the subsystem corresponding to the specified set of components. Thus we will specify a fixed point by a set of components in this paper. For example, $\{1, 2\}$ represents a fixed point with $x_1>0$, $x_2>0$, $x_3=\cdots=x_n=0$, and $\{5\}$ represents $x_5=1$ and $x_i=0$ for $i\neq5$.

It is convenient to introduce a simple nonlinear transformation of the variables when we analyze the flow in the vicinity of the heteroclinic orbits. We will use a logarithmically scaled coordinate, defined as

$$y_i \equiv \log x_i\,. \tag{3}$$

This transformation is valid only for the interior of the phase space, however, it does not cause a serious problem in the analysis of the asymptotic behavior of the orbits because the orbit will stay forever in the interior of the phase space if the initial condition belongs to the interior.

The equation of motion and the constraints are transformed as

$$\frac{d}{dt}y_i=\sum_{j=1}^{n}g_{ij}e^{y_j}-\sum_{j=1}^{n}\sum_{k=1}^{n}g_{jk}e^{y_j}e^{y_k} \tag{4}$$

and

$$\sum_{i=1}^{n}e^{y_i}=1\,,\quad (y_i<0) \tag{5}$$

respectively.

With this coordinate, the asymptotic behavior of the orbit looks like combination of linearly changing segments as shown in Fig. 2. It should also be noted the r.h.s. of (4) is $O(1)$ due to the constraint $y_i<0$. (Here we assumed that $g_{ij}\sim O(1)$. This is generic since we can arbitrarily rescale it by rescaling the time variable.) Thus the change of y_i in a constant duration can be bound uniformly. This is particularly useful property of this equation when we analyze the behavior of the orbits which is asymptotic to the heteroclinic networks as will be seen in the latter part of this paper.

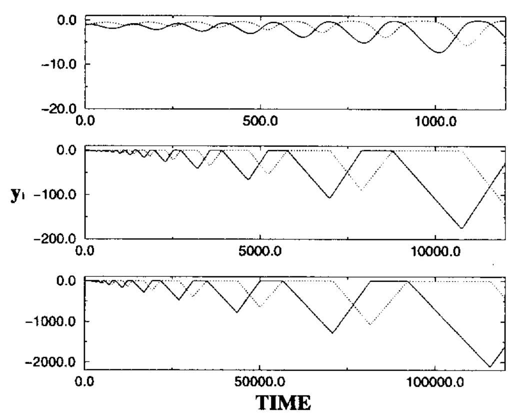

Fig. 2. An example of the orbit being attracted to a heteroclinic cycle (plotted with the transformed variable). This figure corresponds to the same orbit exhibited in Fig. 1, but the ordinate here represents the value of y_i instead of x_i. Note that the 3 boxes have respectively different scales of the ordinate (y_i), which is rescaled in accordance with the scale of time for each box.

A peculiar feature of this system is the existence of the heteroclinic orbits that are persistent against the variation of the parameters. This is basically due to the hierarchical structure of the invariant set of the system described above. Suppose that two saddles A, B and a heteroclinic orbit from A to B exist on an invariant set which corresponds to a subsystem with d components. The heteroclinic orbit will be robust against a small variation of the parameters if

$$\dim A^{u*}+\dim B^{s*}>(d-1), \tag{6}$$

instead of the condition for the case without conserved invariant sets,[16)]

$$\dim A^{u}+\dim B^{s}>(n-1), \tag{7}$$

where A^u and A^{u*} respectively denotes the unstable manifold of saddle A and its restriction to the subsystem. Thus the structurally stable heteroclinic orbits can form a recursive structure which is impossible in a generic case without conserved invariant sets.

In the following analysis, we mainly treat the saddles which are respectively an attractor in a certain subsystem. In this case, the heteroclinic orbit lying in this subsystem is persistent under the variation of the parameters, regardless of the stability of the fixed points related to the other directions. Note that such robust heteroclinic orbits are all lying on the border of the phase space, for it must belong to a certain subsystem.

§ 3. Truncation of the dynamics

3.1. *Preparation*

We will analyze the flow in the vicinity of the network of heteroclinic orbits, with an approximation. Before looking into the detail of the approximation, we will observe the assumption briefly.

There are two basic assumptions as follows. One of them concerns the nature of the flow, and the other poses a restriction for the position in the phase space,

A. All the fixed points should be hyperbolic,

B. The time scale of the stay near the saddles and of the transition between saddles are completely different.

Condition A is satisfied by the generic value for the parameters. And condition B is satisfied by the orbits with typical initial conditions near the heteroclinic orbits at least for some finite duration.

The breakdown of condition B can be caused by two reasons. The first one is caused by an exceptional initial condition which will be mentioned in the analysis. The second comes from the structure of the heteroclinic network. If the network contains a heteroclinic orbit which connects a fixed point saddle and an unstable heteroclinic-cycle, the transition violating condition B occurs for typical initial conditions. However, we do not treat such heteroclinic networks here.

Here we will define the neighborhood of saddle A as the set of points

$$\{\boldsymbol{x}|\max_i|x_i-x_i^A|<\epsilon\}, \tag{8}$$

where x_i^A denotes the value of component x_i at the fixed point A. ϵ is a small positive constant representing the size of the neighborhood.

We will take the neighborhoods sufficiently small, as to satisfy several conditions, i.e., for $\boldsymbol{x}$ belonging to the neighborhood of the saddle A, the conditions

- $x_i^A > 2\epsilon$, if $x_i^A > 0$
- $|\sum_j g_{ij}x_j - \sum_j\sum_k g_{jk}x_jx_k| > \epsilon$, if $x_i^A = 0$

are satisfied. Note that the length of transition between the neighborhoods of two saddles depends on ϵ as $O(|\log\epsilon|)$ for sufficiently small ϵ.

It is convenient to classify the components into two groups, namely, *major* and *minor* ones. We will call such components satisfying $x_i \geq \epsilon$ as major components and the rest as minor ones. Note the obvious fact that $|y_i| < |\log\epsilon|$ for the major components.

3.2. *Derivation of the truncated dynamics*

Since we take the neighborhood small, the flow in the neighborhood of a fixed point is well approximated by the linearized one. The change of y_i during a stay in the neighborhood of a saddle can be approximated by a linear function within a constant error which does not depend on the length of the stay.

From the hyperbolicity of the fixed points, the deviation of each component from the fixed point is smaller than the sum of several monotonically and exponentially changing components which are respectively $\lesssim O(\epsilon)$ throughout the duration. Thus the temporal integration of the deviation of x_i from x_i^A is bound by a constant which is independent of T, and thus the integrated error of $\dot{y}_i$ is also bound by a constant.

Note that, from the definition of ϵ, the total change of y_i is smaller than a constant of $O(|\log\epsilon|)$ for the major components and larger than ϵT for the minor components, where T denotes the length of the stay within the neighborhood.

It should also be noted that the length of transition from a neighborhood of a saddle to another one can be bound by some constant which is $\sim O(|\log\epsilon|)$. Remembering that the order of the change of y_i is at most proportional to the corresponding length of time, we see that the change of y_i in a transition between saddles can be estimated as $O(|\log\epsilon|)$.

Now we will concentrate on the asymptotic behavior of the orbits. We assume here that the typical length of the stays in the neighborhoods of the saddles is sufficiently longer than the length of the transition between the neighborhoods of the saddles. The length of the stays can be arbitrarily long. So we assume that $\epsilon T \gg \epsilon^{-1} \gg |\log\epsilon|$ with T denoting the typical length of the stays. We will consider the truncation of the dynamics for y_i, neglecting the $O(T^0)$ terms. We will use $\boldsymbol{Y}$ to represent the $O(T^1)$ part of $\boldsymbol{y}$ in the following arguments.

First let us consider a stay in the neighborhood of a saddle. From the above arguments, $Y_i = \dot{Y}_i = 0$ for the major components during the stay. On the other hand, $\dot{Y}_i$ for the minor components cannot be neglected because it makes total change of $O(T^1)$ during the stay. The deviation of $\dot{y}_i$ from $\dot{y}_i^A$ makes only the difference of $O(T^0)$ during the stay, thus we will consider $\dot{Y}_i \equiv \dot{y}_i^A$.

The escape from a saddle occurs when one (or more) of Y_i corresponding to the minor component(s) reaches zero. Then the transition to the next saddle will occur within a duration of $O(T^0)$, which causes a change of $O(T^0)$ and thus can be neglected in $\boldsymbol{Y}$. After the transition, $\boldsymbol{Y}$ changes following the value of $\dot{y}_i$ at the next saddle. Note that Y_i never becomes positive since it represents the leading term of y_i which is always negative.

The above sketched kinetics for $\boldsymbol{Y}$ is not closed in the sense that $\dot{\boldsymbol{Y}}$ is not determined from $\boldsymbol{Y}$. We will now look into the relation between $\boldsymbol{Y}$ and $\dot{\boldsymbol{Y}}$ and construct a closed dynamics for $\boldsymbol{Y}$.

Let us consider the behavior of the orbit with an arbitrary initial condition. The orbit will be swiftly attracted to an attractor of subsystem which consists of the components with $Y_i=0$, because the value of x_i component is very small ($\sim O(e^{-\epsilon T})$) if $Y_i<0$ thus the component can be safely neglected for the duration of $O(T)$. There may be some of attractors in the subsystem specified by the initial value of $\boldsymbol{Y}$, however, here we assume that the initially visited saddle is known.

The forthcoming transition generically occurs when one of the minor components (i.e., negative valued component) of $\boldsymbol{Y}$ reaching at zero. Thus the transition path follows the flow of the subsystem with only one additional dimension. Since the previously visited saddle was an attractor in a hyperplane, the number of unstable direction in the phase space is only one. Thus the transition occurs along the unique orbit, thus the next saddle is determined uniquely. In this way, we can determine the arriving saddle from the information of the previous saddle and the value of $\boldsymbol{Y}$, using the structure of the flow. Since the destination of the orbit is an attractor of the subsystem in general cases, we can apply the above argument recursively to obtain the sequence of saddles.

The neighboring saddle at each moment can be determined from the orbit of $\boldsymbol{Y}$ in this way, unless two components of $\boldsymbol{Y}$ simultaneously reach zero. In such cases, the separation of the time scale (between stays and transitions) becomes unclear, and thus there are several possible types of transitions, and the information of $\boldsymbol{Y}$ is not sufficient to determine the final state of this transition. Anyway, it is not generic and we exclude such exceptional cases.

Let us now assume that the staying saddle can be determined from the value of $\boldsymbol{Y}$ at the moment for simplicity. In this case, we can formally write the equation of motion for $\boldsymbol{Y}$ as,

$$\dot{Y}_i=f_i(\boldsymbol{Y})\,. \tag{9}$$

This assumption concerns only the formal simplicity, and the results of the following analysis is also valid even if the relation between $\boldsymbol{Y}$ and staying saddle cannot be written as (9).

3.3. *Further reduction*

Since the function $\boldsymbol{f}(\boldsymbol{Y})$ depends only on whether each component of $\boldsymbol{Y}$ is zero or not, it can be formally expressed as a function of $\boldsymbol{\eta}=\boldsymbol{Y}/|\boldsymbol{Y}|$. Thus, by using the notations

$$\boldsymbol{\eta} \equiv \frac{\boldsymbol{Y}}{|\boldsymbol{Y}|}, \tag{10}$$

$$U \equiv |\boldsymbol{Y}|, \tag{11}$$

$$\boldsymbol{g}(\boldsymbol{\eta}) \equiv \boldsymbol{f}(\boldsymbol{\eta}) - (\boldsymbol{\eta} \cdot \boldsymbol{f}(\boldsymbol{\eta}))\boldsymbol{\eta}, \tag{12}$$

$$h(\boldsymbol{\eta}) \equiv \boldsymbol{\eta} \cdot \boldsymbol{f}(\boldsymbol{\eta}), \tag{13}$$

a set of equations,

$$\frac{d}{dt}\boldsymbol{\eta} = U^{-1}\boldsymbol{g}(\boldsymbol{\eta}), \tag{14}$$

$$\frac{d}{dt}U = h(\boldsymbol{\eta}), \tag{15}$$

is obtained. It should be noted that, there are two constraints on $\boldsymbol{\eta}$, such that,

$$\begin{cases} |\boldsymbol{\eta}| = 1, \\ \max\limits_i \eta_i = 0. \end{cases} \tag{16}$$

We now introduce a dynamically rescaled time variable τ defined as

$$\frac{d\tau}{dt} = U^{-1}. \tag{17}$$

Then Eqs. (14) and (15) can be rewritten as

$$\frac{d}{d\tau}\boldsymbol{\eta} = \boldsymbol{g}(\boldsymbol{\eta}), \tag{18}$$

$$\frac{d}{d\tau}(\log U) = h(\boldsymbol{\eta}). \tag{19}$$

Thus we obtain an autonomous equation for $\boldsymbol{\eta}$. The value of $\boldsymbol{\eta}$ specifies the set of nonzero x_i component at the neighboring saddle. Thus the orbit of $\boldsymbol{\eta}$ determines the sequence of the saddles visited. On the other hand, U determines the time scale of the motion which is associated with the length of the stay near saddles through (17). As can be seen from (17)~(19), the motion in t-coordinate has no characteristic time scale. Steady motion of $\boldsymbol{\eta}(\tau)$ will generically cause a drift of $(\log U)$ with some average velocity measured with τ, which corresponds to a geometrical change of the time scale of the motion in t. Thus a limit cycle solution of (18) corresponds to the sequential visit to several saddles with geometrically changing time scale, that is, an orbit being attracted to (or escaping from) a heteroclinic cycle in the original dynamics.

Since $\boldsymbol{\eta}$ has two constraints (16), the dynamics of $\boldsymbol{\eta}$ corresponds to a semi-flow on an $n-2$ dimensional spherical surface (n is the number of components). Therefore the asymptotic behavior of $\boldsymbol{\eta}$ cannot be irregular if n is smaller than 5. For the system with $n \geq 5$, the dynamics of $\boldsymbol{\eta}$ may be chaotic, as is confirmed in the following analysis.

§ 4. Stability of the heteroclinic cycles

4.1. *Assumptions*

From the argument in the previous section, we see that a chaotic motion of $\boldsymbol{\eta}$, which corresponds to the irregular sequence of saddles, possibly occur in the game dynamics system with 5 or more components. The emergence of such behavior is closely related with the de-stabilization of a heteroclinic cycle attractor. Thus we will analyze the stability and attractivity of heteroclinic cycles in this section. The discussion here is based on the analysis in the previous section, thus we should remember that we are restricting ourselves to the heteroclinic cycles satisfying several conditions, namely,

- Each heteroclinic orbit lies within an invariant hyperplane which corresponds to some subsystem, and the destination of each heteroclinic orbit is an attractor in the subsystem.

From this assumption, an unstable direction is associated with an excitation of a minor component.

- The saddles involved may have two or more unstable directions, however, the heteroclinic orbits which are associated with the excitation of only one of the minor components are considered.

The heteroclinic orbits satisfying the above conditions are common in the game dynamics system. Such orbits always exist, and the recurrent structure like a cycle also exist with fairly large probability. On the other hand, not all of the heteroclinic orbits in the game dynamics system satisfy the conditions. For example, heteroclinic orbits which connects an unstable node in a subsystem and another saddle in the subsystem may exist in the system as likely as the orbits satisfying the conditions.

The reason why we will concentrate on the orbits satisfying the conditions is that those heteroclinic orbits are exclusively relevant for behavior of the orbits in $t \to +\infty$ limit for typical initial conditions as discussed in the previous section. It should be noted that not all the heteroclinic cycles/networks satisfying the conditions are directly related with the asymptotic behavior of the typical orbits, since in many cases the cycles/networks are not attractive. It should be also noted that here we restrict ourselves to the heteroclinic orbits which connects two fixed point saddles. A qualitatively different structure can be observed in the vicinity of the heteroclinic network with a heteroclinic orbit which connects a fixed point and a heteroclinic cycle.

4.2. *Return map*

Here we will analyze the dynamics with a return map on a Poincaré section. Let us consider a surface of section which corresponds to an exit of a saddle, i.e., a surface which intersect with a heteroclinic orbit starting from the saddle. The section corresponds to the moment that the value of a certain minor component x_l reaches ϵ

after the stay in the saddle, i.e., the moment that Y_I reaches zero.

From the property of the dynamics of $\boldsymbol{Y}$, we can neglect the variation of $\boldsymbol{Y}$ during the transition between the neighborhoods of the saddles, and thus the return map for $\boldsymbol{Y}$ on the surface of section can be expressed as a product of 1-saddle maps that respectively represent the change of $\boldsymbol{Y}$ in the neighborhood of a saddle.

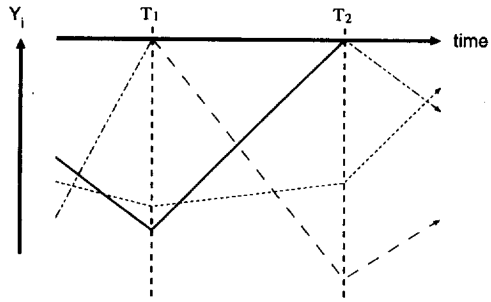

Fig. 3. Schematic illustration for 1-saddle map. This figure shows the change of $\boldsymbol{Y}$ schematically. T_1 represents the time when the orbit arrives at the saddle in question, and T_2 is the time to leave from the saddle. $\boldsymbol{Y}^{\text{in}}$ and $\boldsymbol{Y}^{\text{out}}$ in the text correspond to $\boldsymbol{Y}(T_1)$ and $\boldsymbol{Y}(T_2)$ in this figure.

Since the change of $\boldsymbol{Y}$ during a stay in the neighborhood of a saddle can be regarded as linear, the total change of $\boldsymbol{Y}$ in a stay can be calculated easily. Let us use $\boldsymbol{Y}^{\text{in}}$, $\boldsymbol{Y}^{\text{out}}$ for the value of $\boldsymbol{Y}$ at the entrance and exit of the saddle and $\boldsymbol{\lambda}$ for the value of $\dot{\boldsymbol{Y}}$ at this saddle (see illustration in Fig. 3). Then the relation between $\boldsymbol{Y}^{\text{in}}$ and $\boldsymbol{Y}^{\text{out}}$ can be written as

$$Y_i^{\text{out}} = -\frac{\lambda_i}{\lambda_I} Y_I^{\text{in}} + Y_i^{\text{in}}, \tag{20}$$

where I denotes the component which is associated with the escaping direction in consideration. Since Y_i^{out} must not be positive, $\boldsymbol{Y}^{\text{in}}$ must satisfy a condition in order for (20) to be valid if the considering saddle has 2 or more of the unstable directions. The condition is expressed as a set of inequalities between relative ratios of the components of $\boldsymbol{Y}^{\text{in}}$. It should be noted that the map can be calculated from g_{ij}; the value of x_i at a fixed point as well as the growth rate at the point can be determined from the matrix.

As we have seen above, the return map can be expressed as a sequential product of 1-saddle maps, which is respectively a linear map. Thus the return map for $\boldsymbol{Y}$ is a linear map, which is defined on a restricted region if the cycle contains saddles with two or more unstable directions. The defined region of the return map may vanish, if the specified sequence of the saddles is not realized by typical initial conditions.

4.3. *Stability of the heteroclinic cycle, and the properties of the return map*

The 'stability' condition of the heteroclinic cycle can be expressed with the eigenvalues and eigenvectors of the matrix representing the return map. The analysis of this return map does not say anything concerning the orbits which do not belong to the defined region of the map. Therefore it should be noted that the argument presented below concerns the stability in a weak sense (*relative* asymptotic stability introduced by Ura[17),7)]).

The condition that the orbit does not run away by the iteration of the return map can be expressed as follows.

1. an eigenvector of the matrix must exist in the defined region of the return map.

2. the corresponding eigenvalue should have the largest amplitude among the eigenvalues of the matrix.

For the heteroclinic cycle to be attractive, an additional condition is required, i.e.,

3. the eigenvalue should be larger than 1.

Since if the eigenvalue is smaller than 1, the iteration makes the $|\boldsymbol{Y}|$ smaller, that is, the orbit diverges gradually from the heteroclinic cycle. (Note that the eigenvector always corresponds to a positive eigenvalue if it is in the well-defined region of the map, since the return map never changes the sign of Y_i.)

If the heteroclinic cycle contains saddles with two or more unstable directions, the defined region of the return map is restricted, indicating that there exists a set of initial conditions in the arbitrary small neighborhood of the heteroclinic orbit which escapes from the cycle. Thus the heteroclinic cycle is not asymptotic stable, although it can be an attractor if conditions $1\sim3$ are satisfied.[9)]

Another strange phenomenon occurs when condition 2 alone is broken. In this case, though the heteroclinic cycle no longer is an attractor, there still exists a set of initial conditions with zero measure which will be attracted to the heteroclinic cycle.

If $\boldsymbol{Y}$ has a value outside of the region of definition of the return map, the orbit will get apart from the cycle at some saddle with two (or more) unstable directions. The destination of the orbit which escapes from the cycle depends on the global structure of the flow, however, the sequence of saddle can be determined as a function of the initial value of $\boldsymbol{Y}$ anyway. In some cases, the orbit returns to the surface of section again. In such cases we can extend the return map for the value outside of the region of definition of the return map along the cycle. In this way, the return map on this surface of section is obtained as a patchwork of linear maps. We will investigate an example of the extended return map in the next section. Note that there might exist some runaway regions, i.e., the set of $\boldsymbol{Y}$ corresponding to the orbits which never return to this surface of section.

§ 5. Analysis on an example system

5.1. *Parameters of the system*

In this section, we will apply the above-mentioned analysis on a specific example system, and also present the corresponding results of numerical simulations.

The example system is a game dynamics system with 5 components and parameter values are set as

$$g_{ij}=\begin{pmatrix} -1.0 & -20.0 & -0.4 & -1.0 & 1.0 \\ 1.5 & 0.0 & -0.7 & -7.3 & 0.5 \\ X & 1.0 & 0.0 & 0.0 & -0.1 \\ -0.9 & 0.8 & 1.0 & -1.0 & -0.1 \\ 0.0 & -8.0 & 0.7 & 1.3 & 0.0 \end{pmatrix}, \tag{21}$$

where $X(g_{31})$ is set as several different values in the following analysis to observe the

Table I. Examples of the recursive paths to the Poincaré section.

	sequence of the saddles
C1	$\{3,4\}\to\{5\}\to\{1,5\}\to\{2\}\to\{3\}\to\{5\}\to\{2\}\to\{3\}\to\{3,4\}$
C2	$\{3,4\}\to\{5\}\to\{1,5\}\to\{2\}\to\{3\}\to\{3,4\}$
C3	$\{3,4\}\to\{5\}\to\{2\}\to\{3\}\to\{3,4\}$

bifurcation concerning the stability of the heteroclinic cycles and the emergence of the chaotic rambling orbits.

5.2. *Return map for* $\boldsymbol{Y}$

First we will concentrate on the stability of heteroclinic cycle C2, illustrated in Table I. The Poincaré surface of section is taken at the transition between $\{3,4\}\to\{5\}$.

From the property of the truncated dynamics, $\boldsymbol{Y}$ has three zero-components at the surface of section, namely, Y_3, Y_4 and Y_5. Also from the discussion on the return map associated with a heteroclinic cycles, we know that the return map is linear. Thus the return map on the surface of section can be represented with a 2×2 matrix.

The matrix is calculated as a product of several 1-saddle maps with form of (20) and thus can be determined from $\{g_{ij}\}$. As a result we obtain a representation for the return map as

$$\begin{pmatrix} Y_1 \\ Y_2 \end{pmatrix} \to \begin{pmatrix} 1.9389+6.418X & 1.2386-12.836X \\ 2.841+8.42X & 0.634-16.84X \end{pmatrix} \begin{pmatrix} Y_1 \\ Y_2 \end{pmatrix} \tag{22}$$

with an restriction on the initial value of $\boldsymbol{Y}$,

$$\frac{4.28X-0.078}{2.14X+0.747} < \frac{Y_1}{Y_2} < 2.0\,. \tag{23}$$

Since the original flow has 4 degrees of freedom, the return map should be 3-dimensional in general. Thus it is surprising that we have 2-dimensional map here. The extra reduction comes from the strong dynamical contraction.

The contraction/expansion of the deviation of y_i is very slow except while y_i is a major component. (It is because $\partial \boldsymbol{y}/\partial y_i \sim O(\exp y_i)$.) Thus the contraction at saddles $\{3,4\}$ and $\{1,5\}$, which makes the strong contraction of order $O(e^{-\epsilon T})$ for one direction perpendicular to the orbit, is the only change which has exponential dependence on T. The contraction/expansion in the rest of the directions is much slower than this contraction; it is multiplied by some factor for each turn of the cycle. Thus we can drop one extraneous dimension by the dynamical contraction in the large T limit.

As is discussed previously, the heteroclinic cycle becomes an attractor if some conditions on the eigenvalues and eigenvectors of the matrix representing the return map are satisfied. In the considered range of the parameter value, the two eigenvalues are respectively positive (>1) and negative, and the eigenvector corresponding to the positive eigenvector stay within the region (23). Thus conditions 1 and 3 are satisfied.

The critical value of X for the condition 2 is given by

$$\mathrm{Trace}(M^{C2}) = 2.5729 - 10.422X = 0\,, \tag{24}$$

where M^{C2} represents the matrix in (22). This condition gives the critical value $X_c = 0.247\cdots$. If X exceeds X_c, the absolute value of the negative eigenvalue exceeds the positive one, and thus the typical orbit will escape from the cycle C2.

5.3. *Reduced return map*

Before considering the behavior of the orbits which escape from the cycle, we will consider the reduction of the return map (22).

As is given in the previous section, the dynamics of $\boldsymbol{Y}$ can be separated into two components, namely, the dynamics of the direction and the dynamics of the amplitude. The latter does not affect the former except for the speed of the motion. Thus we can reduce the return map by separating the amplitude part.

Here we analyze the return map with projection to $Y_2 = 1$ instead of $|\boldsymbol{Y}| = 1$. Thus the return map for the direction of $\boldsymbol{Y}$ can be reduced to a one-dimensional map, using

$$Z \equiv Y_1 / Y_2. \tag{25}$$

The concrete form of the map is,

$$Z \mapsto f^{C2}(Z) = \frac{(6.418X + 1.9389)Z - 12.836X + 1.2386}{(8.42X + 2.841)Z - 16.84X + 0.634} \tag{26}$$

and it is defined for a range of Z satisfying

$$\frac{4.28X - 0.078}{2.14X + 0.747} < Z < 2.0\,. \tag{27}$$

From the nature of the return map for $\boldsymbol{Y}$, we can confirm that the attractor vanishes from this region when the fixed point becomes unstable; Since the map for $\boldsymbol{Y}$ is linear, it is obvious that there are no non-linear terms which suppress the growth of the deviation from the eigenvector. Thus, if X is slightly larger than X_c, the orbit which is initially in the region of C2 eventually escapes from this cycle. The escaping orbit, however, eventually returns to the surface of section through the path indicated as C3 in Table I. The return map for Z corresponding to the path C3 becomes

$$Z \mapsto f^{C3}(Z) = \frac{Z + 3.1164}{6.316}\,. \tag{28}$$

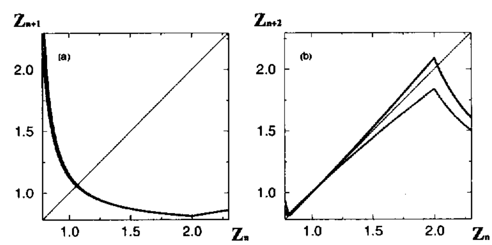

Fig. 4. Return maps for Z with X slightly above and below the bifurcation point $X = X_c$. (a) and (b) exhibit respectively the first- and second-return map on the surface of section described in the text. Each curve in the figures represents the return map for Z calculated from the truncated dynamics. The solid lines correspond to $X = 0.25$ which is slightly above X_c (chaotic), and the dotted lines correspond to $X = 0.24$ below X_c (regular). The bifurcation at $X = X_c$ is similar to the bifurcation in the tent map, as is seen from (b).

The range of Z corresponding to this path is

$$Z > 2.0\,. \tag{29}$$

The first- and second-return map corresponding to the parameter X slightly larger than and smaller than X_c is displayed in Fig. 4. The second return map exhibits the de-stabilization of the fixed point clearly. As is obvious from the shape of the return map, the orbit of this map will be attracted to a chaotic attractor when X is slightly larger than X_c, and then the chaotic sequence of the mixture of C2 and C3 will be created.

The information of the amplitude part of $\boldsymbol{Y}$ is omitted in this return map. We can calculate the average magnification rate of $\boldsymbol{Y}$ per one cycle by taking the average on the natural invariant measure of the return map. Although the exact calculation is complicated, we can easily confirm that it is larger than 1. Therefore the amplitude of $\boldsymbol{Y}$ eventually grows with some average growth rate. It implies that the corresponding orbit of the original system (1) eventually approaches the heteroclinic network and the typical length of stays will grow exponentially on average.

5.4. *Results of numerical simulations*

Here we will exhibit the results of numerical simulations on the system with $X = 0.24$, 0.25 and 0.32. The specific features of the algorithm used in the simulation is briefly summarized in Appendix A.

First the sequence of saddles is exhibited in Fig. 5. The abscissa represents the logarithm of the time and the ordinate shows the visiting saddle. In box (a) the orbit being attracted to a stable heteroclinic cycle is exhibited. In box (b), a subharmonic like oscillation is apparent, however, from the close inspection, we can observe the orbit fluctuating chaotically as is predicted by the analysis. In box (c), the oscillation becomes much more disordered, and the period 2 like structure observed in (b) is broken.

Figure 6 shows the variation of the length of stays. The logarithm of the length of stays is plotted in sequentially order of the visit. The logarithm of the length of the stay grows approximately linearly with the number of visited saddles. For all of these three cases, the dots roughly ride on a straight line, in-

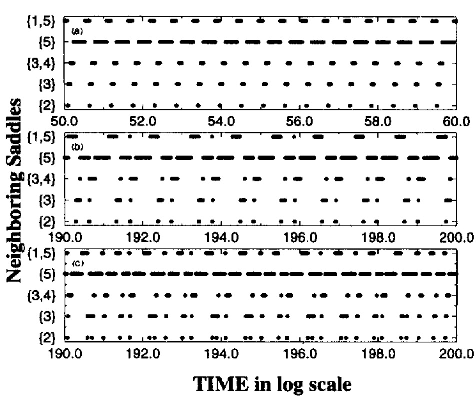

Fig. 5. Three examples of the sequence of saddles. These figures exhibit the sequence of saddles which corresponds to the numerically obtained orbits of the game dynamics system with 5 components with parameters given by (21). The value of X is set as 0.24 for (a), 0.25 for (b) and 0.32 for (c). The abscissa represents the *logarithm* of the time, and the ordinate shows the neighboring saddle. The initial condition is set as $x_1 = x_2 = \cdots = 0.2$ for all cases. (a) exhibits the regular oscillation with geometrically expanding period. (b) seems regular too, however, it is not completely regular as can be seen from the irregular visits to saddle $\{1, 5\}$. The irregularity is more obvious in (c).

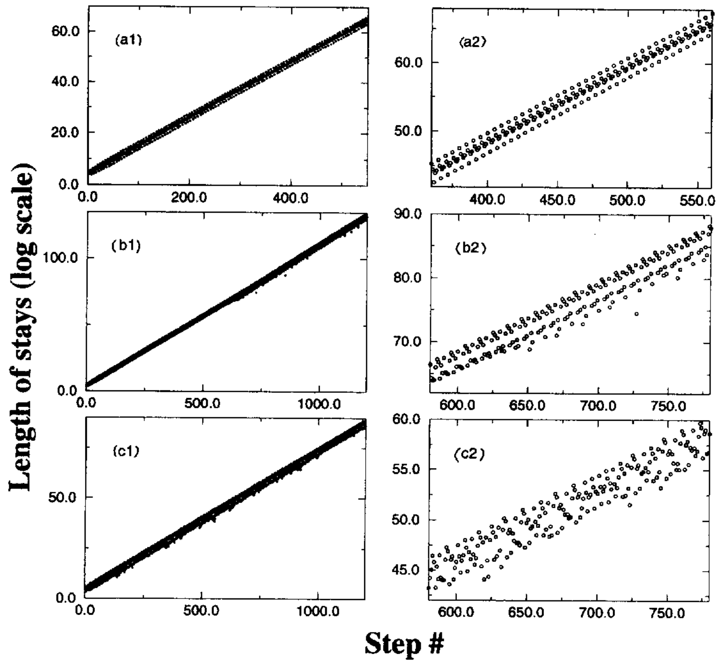

Fig. 6. Variation of the lengths of the stay near saddles. The dots are sorted from left to right according to the sequential order of the visit, and the ordinate represents the logarithm of the length of the stay in the neighborhood of saddles with radius $\epsilon=10^{-8}$. Each pair of boxes ((a1) and (a2), etc.) correspond to an orbit in Fig. 5 and thus plotted from the same data.

dicating that the variation of the length of the stays is geometric, at least on average. However the detail of the sequence has qualitative difference. In Fig. 6 (a), the sequence of the length of the stays has a regular structure. On the other hand, in Figs. (b) and (c), we can see an irregular fluctuation. Since the dynamics itself is completely deterministic, the irregular fluctuation is naturally associated with intrinsic chaotic dynamics. Note that the geometric variation of the length of stays is fairly universal and is observed even if the heteroclinic cycle/network is repulsive. In this case, the length of stays decreases in a geometrical manner until it diverges away from the heteroclinic cycle/network.

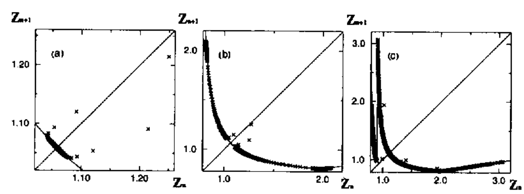

Fig. 7. Numerically obtained return maps. The marks in the figures show the value of y_1/y_2 for two successive intersections of an orbit and a surface of section. (a)~(c) correspond to the three orbits in Fig. 5. The surface of section is taken as $x_5=\epsilon$ with restriction to $x_3>\epsilon$, $x_4>\epsilon$, $\dot{x}_5>0$ ($\epsilon=10^{-8}$). The solid curves represent the analytically calculated return map for Z for the corresponding parameter values. The marks and the solid lines match well except for initial transients corresponding to the early stage before the orbit approaches the heteroclinic orbits enough.

Finally, we will examine the behavior of the orbit with a return map by observing the quantity corresponding to Z. Here we will take the surface of section as $x_5=\epsilon$, $x_3>\epsilon$, $x_4>\epsilon$, $x_1<\epsilon$, $x_2<\epsilon$, with $\epsilon=10^{-8}$, and plot the value of y_1/y_2 for the successive two visits to this surface of section. Figure 7 shows the results. The solid lines in the figure shows the return map for Z obtained from the analytical calculation, and the marks show the numerical results.

As can be seen from (b), the orbit moves along the path C2 for relatively many turns before it escapes from C2. This relatively long transient motion can also be observed in Figs. 6 (b1) and (b2), before about 650th saddle. The orbit is eventually attracted to the chaotic attractor and visits two bands, $1.89\cdots < y_1/y_2 < 2.09\cdots$ and $0.81\cdots < y_1/y_2 < 0.825\cdots$, in tern. In case (c), the attractor becomes much more larger and the marks spread over $0.81\cdots < y_1/y_2 < 3.1\cdots$. The attractor contains three possible recurrent paths listed in Table I.

In any case, the marks are distributed well along the lines except for a relatively small number of initial transients corresponding to the early stage. Thus we confirm that the truncation gives good approximation for these cases.

§ 6. Summary and discussion

We have analyzed the dynamics in the vicinity of a heteroclinic network with a simple approximation, which is valid if the stay near the saddle is sufficiently long in relative to the transition between saddles. The analysis shows that the typical motion in the neighborhood of the heteroclinic network has no characteristic time scale. The analysis also implies the existence of the new type of asymptotic behavior. In this case, typical orbits are attracted to a heteroclinic network with a branching structure, repeatedly visiting several saddles with irregular order. The irregularity of the motion is associated with a deterministic chaos. Thus the orbit rambles over several saddles with a chaotic order, and with irregular but on average exponentially expanding length of the stays. The existence of such orbits is also observed in the numerical simulation.

The analysis presented in this paper is based on the structure of the network of heteroclinic orbits, and the specific form of the interaction is not essential. The existence of such structure is enabled by the hierarchical structure of the invariant set, which comes from the form of the equation as

$$\dot{x}_i = x_i f_i(\boldsymbol{x}) . \tag{30}$$

Thus the essential part of the analysis is expected to be valid for the flow in the vicinity of the networks of heteroclinic orbits in the systems expressed by the equation of the above form. Many of the systems with symmetry can be represented in such form, and consequently we can expect that the chaotic sequence of quasi stable states can be observed in the behavior of the model systems with adequate symmetry.

We have been restricted ourselves to the heteroclinic networks with relatively simple geometry. The structure of the network can be more complicated, and correspondingly more complicated dynamical behavior occurs in the vicinity of such heteroclinic networks as will be reported in a forthcoming paper.

Acknowledgements

The author is grateful to S. Sasa for extensive discussion and collaboration in related works. He also thanks Y. Kuramoto for enlightening advice, and T. Ikegami, H. Tanaka, T. Yanagida, K. Kaneko and K. Okuda for valuable suggestions. Thanks are also due to T. Shichijo and K. Watanabe for collaboration in an earlier stage of this study, and to G. C. Paquette for the careful reading of the earlier version of this manuscript. This work was supported by the Yukawa foundation.

Appendix
—— *Algorithm for the Numerical Simulation* ——

Although the form of Eq. (1) is quite simple, there are some difficulties in tracing the orbit of this system numerically because of the limited precision of the calculation, especially when the orbits are in the vicinity of the heteroclinic orbits. Thus the algorithm used for the simulation has several specific features as listed below.

1. The calculation is carried out using the transformed variables, i.e., we used (4) instead of (1).
2. The step size of the calculation is controlled adaptively.
3. Constraint (2) is realized dynamically.

The transformed variables are used in order to avoid the loss of very small deviation from the heteroclinic orbits which may be caused by the underflow. Since the heteroclinic orbits considered in this paper are lying on the border of the phase space ($x_i=0$ for some components), the trace of the very small deviation is enabled by the transformation concerning the minor components. On the other hand, the small deviation in the direction of major components is not saved by this transformation, thus we still lose the information about the small deviation of those components. Fortunately enough, however, because of the strong dynamical contraction in the direction of the major components at related saddles, the deviation in those components does not cause considerable effects on the behavior of orbits. In this way, we can calculate the behavior of the orbits with a fairly good precision by using this transformation.

As is discussed in the main part of this paper, the target behavior consists of a long stay near the saddles and transitions between saddles which are relatively swift. Thus the adaptive control of the step size is indispensable for the simulation of the orbit in a realistic length of calculation. The used algorithm is the Runge-Kutta method and we kept the precision of the calculation as 10^{-8} in the growth rate $\dot{y}_i$.[18]

We will then observe on the algorithm for the realization of the constraint (2). Taking the sum of (1) over i, we obtain

$$\begin{aligned}\frac{d}{dt}\Big(\sum_i x_i\Big) &= \sum_i\sum_j g_{ij}x_ix_j - \sum_i x_i \sum_j\sum_k g_{jk}x_jx_k \\ &= \Big(\sum_j\sum_k g_{jk}x_jx_k\Big)\Big(1-\sum_i x_i\Big)\,. \end{aligned} \tag{A1}$$

Therefore, if $\sum_{i,j} g_{ij} x_i x_j > 0$ is satisfied, then $\sum_i x_i$ will converge to 1.

On the other hand, the flow on the surface $\sum x_i = 1$ is not changed by the transformation of adding constant to all components of $\{g_{ij}\}$, i.e.,

$$g_{ij} \mapsto g_{ij} + C\,, \tag{A2}$$

where C is an arbitrary real number which is independent of i and j.

Therefore we can control the value of $\sum g_{ij} x_i x_j$ by the adaptive control of the value of C. We thus realize the constraint (2) by controlling C dynamically.

References

1) R. M. May and W. J. Leonard, SIAM J. Appl. Math. **29** (1975), 243.
2) P. Ashwin and J. W. Swift, J. Nonlinear Science **2** (1992), 69.
3) K. Okuda, Thesis, Kyoto Univ. (1994).
4) E. Knobloch and M. Silber, Physica **D63** (1993), 213.
5) D. Hansel, G. Mato and C. Meunier, Phys. Rev. **E48** (1994), 3470.
6) J. Guckenheimer and P. Holmes, Math. Proc. Camb. Phil. Soc. **103** (1988), 189.
7) W. Brannath, Nonlinearity **7** (1994), 1367.
8) V. Kirk and M. Silber, Nonlinearity **7** (1994), 1605.
9) I. Melbourne, Nonlinearity **4** (1991), 835.
10) P. D. Taylor and L. B. Jonker, Mathematical Bioscience **40** (1978), 145.
11) M. Eigen, Naturwissenschaften **58** (1971), 465.
12) J. Hofbauer and K. Sigmund, *The Theory of Evolution and Dynamical Systems* (Cambridge University Press, 1988).
13) J. Hofbauer, Nonlinear Analysis **5** (1981), 1003.
14) M. E. Gilpin, Amer. Nat. **113** (1979), 306.
15) A. Arneodo, P. Coullet and C. Tresser, Phys. Lett. **79A** (1980), 259.
16) J. Guckenheimer and P. Holmes, *Nonlinear Oscillations, Dynamical Systems, and Bifurcations of Vector Fields* (Springer-Verlag, New York, 1983).
17) T. Ura, *Contributions to Differential Equations*, vol. **3**, No. 3 (New York, Wiley, 1964), p. 249.
18) W. H. Press, B. P. Flannery, S. A. Teukolsky and W. T. Vetterling, *NUMERICAL RECIPES in C* (Cambridge University Press, 1988).